Thermochimica Acta, 216 (1993) 107–117
Elsevier Science Publishers B.V., Amsterdam

New oxygen or nitrogen carriers

A. Busnot *, J.F. Le Querler and J. Yazbeck

Laboratoire de Chimie Minérale et Bioinorganique, U.F.R. de Sciences, Université de Caen, 14032 Caen Cedex (France)

(Received 10 July 1992)

Abstract

Complexes of nickel(II) with the composition $Ni_vO_w(Imid)_xA_y \cdot zNH_3$ or $Ni_{v'}N_{w'}(Imid)_{x'}A_{y'} \cdot z'NH_3$, where Imid represents the imidazole molecule and A the anion of aspartic acid, picolinic acid, glutaric and glutamic acids, *N*-acetylglycine or histidine, have been synthesized. The results of thermal and spectral studies are analysed for the various complexes. The TGA curves and diffuse reflectance spectra are reported. Calculated electronic transitions are in good agreement with those observed. The monomeric or dimeric character of these complexes is shown. The nickel ions seem to be in an octahedral environment.

INTRODUCTION

The utilization of molecular oxygen in biological systems is obviously of extreme importance. The ability of transition metal ions to reversibly coordinate O_2 has been known for a long time. Some of the first synthetic systems reported to bind O_2 were cobalt(II) complexes [1]. Monomeric Co(II)–dioxygen adduct complexes are of chemical and biological interest [2]. Much of the recent activity in this area has been motivated by a desire to elucidate the factors which lead to reversible O_2 binding and to understand the transport of O_2 and oxidation by O_2 in biological systems.

In addition to their significance as models [3] of natural oxygen carriers, synthetic dioxygen complexes have potential applications in dioxygen separation and storage [4], industrial processes [5, 6] and catalysis [7]. Interest in the catalytic aspects of dioxygen complexes has intensified in recent years [8]. These complexes promote reactions similar to or identical to those promoted in biological systems [9, 10].

Recently, several oxygen-carrying chelates containing coordinating ions other than cobalt have been reported [10, 11]. Accordingly, we have directed our initial efforts toward a study of these complexes.

* Corresponding author.

EXPERIMENTAL AND RESULTS

Complexes involving Ni(II) aspartate, Ni(II) picolinate, Ni(II) *N*-acetylglycinate, Ni(II) histidinate, Ni(II) glutarate, Ni(II) glutamate and imidazole have been prepared.

A mixture of imidazole and nickel sulfate in ammoniacal medium was stirred and filtered. The solution was kept under an O_2 or N_2 flow for 5 min

TABLE 1

Microanalysis results

Compound	Element	Theoretical (wt.%)	Experimental (wt.%)
A	C	37.8	37.4
	H	5.3	5.4
	N	27.2	27.1
	Ni	9.5	9.4
B	C	38.0	
	H	5.4	
	N	31.9	
	Ni	9.5	9.7
C	C	45.7	46.0
	H	3.8	4.2
	N	17.8	17.8
	Ni	12.4	11.8
D	C	44.4	
	H	3.7	
	N	23.0	
	Ni	12.0	11.7
E	C	32.6	32.7
	H	6.6	5.1
	N	25.3	25.5
	Ni	8.8	8.7
F	C	37.7	37.9
	H	5.6	5.4
	N	27.1	27.3
	Ni	9.4	9.6
G	C	38.7	38.0
	H	6.2	5.5
	N	26.9	26.0
	Ni	9.0	9.1
H	C	33.7	35.1
	H	6.4	5.4
	N	24.7	26.3
	Ni	9.4	9.6

and filtered. The solution obtained was heated with the dicarboxylic acid and left at 278 K to reach crystallization. The following compounds were obtained: **A**, $NiO_2(Imid)_9(aspartate)_3(NH_3)_3$; **B**, $Ni_2N_4(Imid)_9$-$(aspartate)_3(NH_3)_3$; **C**, $NiO_2(Imid)_2(picolinate)_2$; **D**, $NiN_2(Imid)_2$-$(picolinate)_2$; **E**, $NiO_2(Imid)_2$(N-acetyglycinate)$_3(NH_3)_5$; **F**, $Ni_2O_4(Imid)_2$-$(histidine)_6(NH_3)_4$; **G**, $Ni_2O_4(Imid)_9(glutarate)_3(NH_3)_7$; **H**, $Ni_2O_4(Imid)_5$-$(glutamate)_4(NH_3)_8$.

The results of quantitative elemental analyses (Table 1) for all the above mentioned complexes support the formulae given above.

THERMAL STUDIES

Additional studies were carried out by thermogravimetry to confirm the molecular formulae assumed on the basis of elemental analysis. The measurements were performed in air over the temperature range 293–1293 K at a heating rate of 10 K min^{-1} using a Setaram TG 85 microbalance.

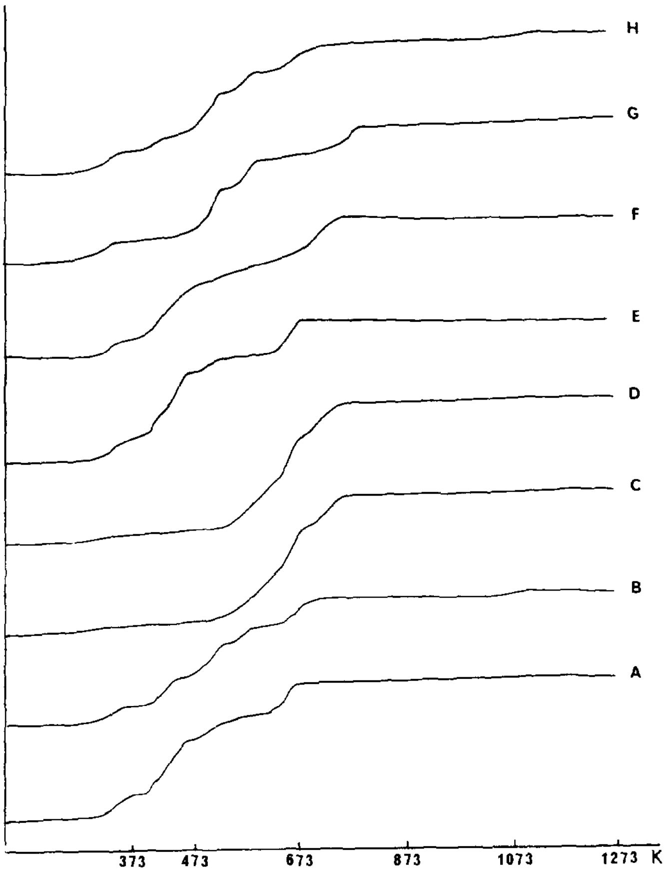

Fig. 1. TG curves in air.

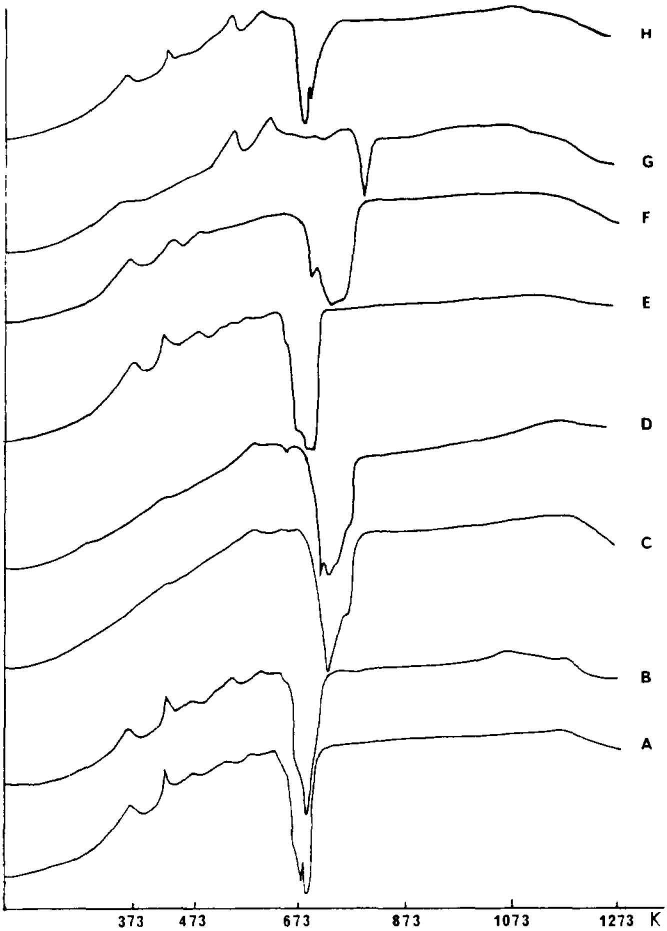

Fig. 2. Thermal differential curves in air.

Thermoanalytical diagrams for the complexes are shown in Figs. 1 and 2. The final stage of the decomposition forms the nickel oxide for all compounds studied. The general scheme of decomposition of the different complexes is summarized in the mechanisms shown in the Appendix (WL = weight loss). The intermediate compounds in the Appendix were assumed but not isolated.

DIFFUSE REFLECTANCE SPECTRA

Diffuse reflectance spectra were recorded at room temperature for all compounds on a Beckmann UV 5240 spectrophotometer over the range 40 000–4000 cm^{-1}. Kodak white reflectance standard was used as a reference for the dilution of nickel samples (10 wt.%).

In the near IR sharp peaks of weak intensity correspond to harmonics and combination bands of fundamental vibrations of the ligands. These

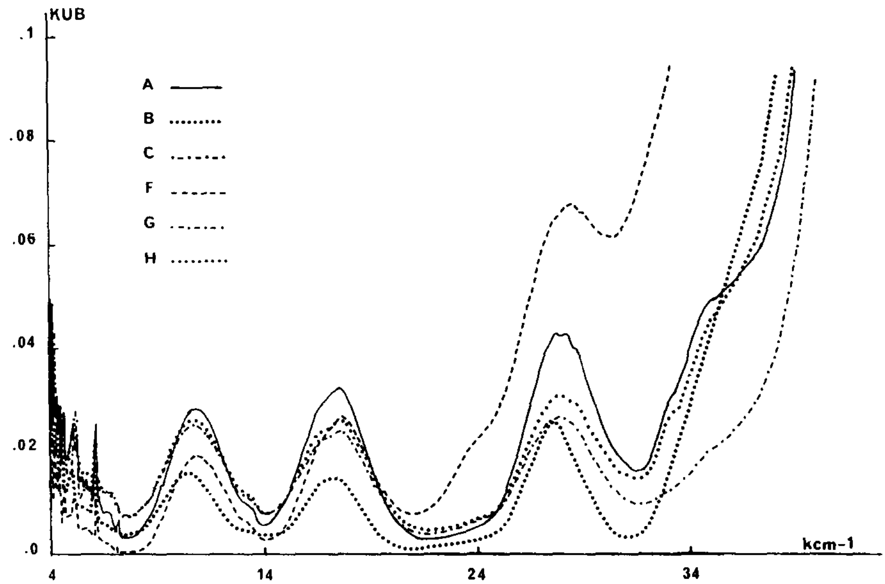

Fig. 3. Reflectance spectra.

bands are very difficult to assign. Various types of spectra were recorded and these are shown in Figs. 3 and 4. The electronic transitions observed and calculated for the different compounds are shown in Table 2.

The ground state observed is ${}^3A_{2g}$. The principal band ν_2 around 17 500 cm^{-1} is due to the ${}^3A_{2g}(F) \rightarrow {}^3T_{1g}(F)$ transition. A ν_1 band near 10 750

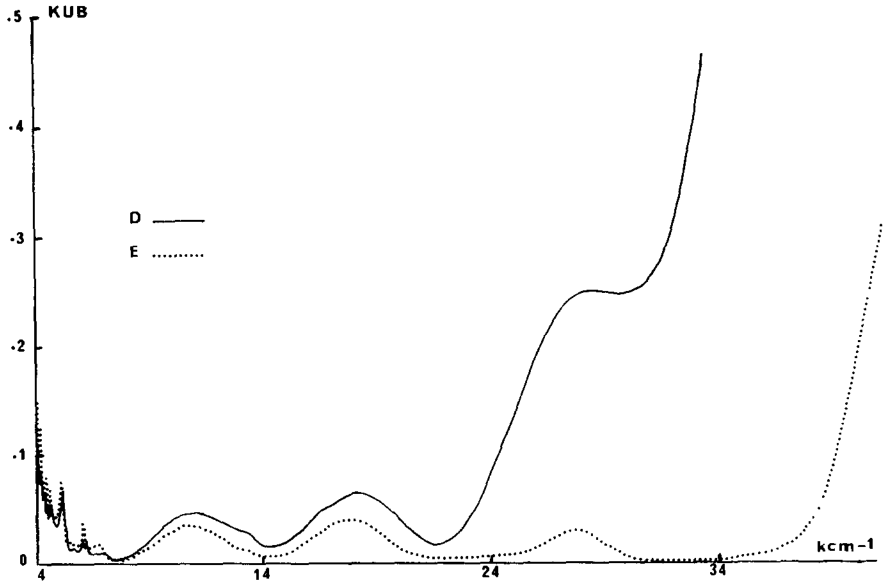

Fig. 4. Reflectance spectra.

TABLE 2

Electronic transitions (cm^{-1}) observed and calculated for the various complexes

Transition	Compound							
	A	B	C	D	E	F	G	H
ν_1								
Exp.	10 666	10 656	10 905	10 881	10 651	10 864	10 719	10 627
Calc.	10 485	10 390	10 776	11 084	10 969	10 778	11 000	10 429
$^3A_{2g}(F) \rightarrow {}^3T_{2g}(F)$								
Shoulder								
Exp.	13 286	13 120	13 120	13 179	13 381	13 328	13 325	13 286
Calc.	13 762	13 637	13 721	13 692	13 776	13 802	13 400	13 822
$^3A_{2g}(F) \rightarrow {}^1E_g(D)$								
$\nu_3^* - \nu_1$								
Exp.	16 985	16 696	17 504	17 436	17 000	17 056	17 091	17 183
Calc.	16 941	16 787	17 248	17 236	17 092	17 502	16 562	17 107
$^3T_{1g}(P) \rightarrow {}^3A_{2g}(F)$								
ν_2								
Exp.	17 413	17 280	18 016	17 957	17 492	17 632	17 636	17 492
Calc.	17 165	17 326	17 644	17 955	17 602	17 813	17 039	17 343
$^3A_{2g}(F) \rightarrow {}^3T_{1g}(F)$								
Shoulder								
Exp.	23 762		23 603		22 413	23 172		22 810
Calc.	23 421		22 986		22 704	23 430		22 692
$^3A_{2g}(F)\,{}^1T_{2g}(P)$								
ν_3^*								
Exp.	27 651[a]	27 352[a]			27 651[a]	27 920[a]	27 330	27 810[a]
Calc.	27 426	27 177			28 061	28 280	27 157	27 536
$^3A_{2g}(F) \rightarrow {}^3T_{1g}(P)$								
ν_3^*								
Exp.	28 127		28 409[a]	28 317[a]	28 160	29 040	27 810[a]	
Calc.	27 772		28 024	28 320	28 571	28 610	27 562	
$^3A_{2g}(F) \rightarrow {}^1T_{1g}(G)$								
Imidazole								
Exp.	33 048					32 512		33 206
Calc.	32 950					32 950		32 950
Exp.	35 024						35 270	34 952
Calc.	35 070						35 764	35 010
$^3A_{2g}(F) \rightarrow {}^1E_g(G)$								
D_q (cm^{-1})	1117	1106	1159	1151	1122	1128	1135	1121
B (cm^{-1})	770	763	777	783	766	781	760	778

[a] ν_3 frequency used to calculate D_q and B in the relations $340D_q^2 - 18(\nu_2 + \nu_3^*)D_q + \nu_2\nu_3^* = 0$, $B = \dfrac{\nu_3^* + \nu_2 - 30Dq}{15}$ (see explanations in ref. 11).

is due to the $^3A_{2g}(F) \rightarrow {}^3T_{2g}(F)$ transition. We observed a ν_3 band, which appears for all the complexes near 28 000 cm^{-1}, due to the $^3A_{2g}(F) \rightarrow {}^3T_{1g}$(P or G) transitions.

This assignment seems to be in accord with the various transitions observed. A shoulder at around 13 250 cm^{-1} appears to be due to a spin-forbidden transition. It is possible that ligand field in these complexes is distorted from true octahedral symmetry and that the low symmetry component splits the $^3A_{2g}(F) \rightarrow {}^3T_{2g}(F)$ transition, giving the spin-allowed band $^3A_{2g}(F) \rightarrow {}^1E_g(D)$. The Racah parameter B [12] can be deduced for a d_8 ion if Δ_0 is the energy of the first transition, the Δ_0/B [13] value leads to the position of each transition. The predicted transition values are in good agreement with the observed values and it seems that the octahedral environment of the complexes is not affected by the nature of the oxygen or nitrogen molecules, or by the imidazole ligand.

REFERENCES

1 R.H. Bailes and H. Calvin, J. Am. Chem. Soc., 69 (1947) 1886.
2 R.D. Jones, D.A. Summerville and F. Basolo, Chem. Rev., 79 (1979) 139–179.
3 N.M. Semozan, J. Chem. Educ., 51 (1974) 503.
4 A.J. Adduci, Chemtech., 6 (1976) 575.
5 J.S. Valentine, Chem. Rev., 73 (1973) 235.
6 C.A. MacAuliffe, H.Al. Khatech, M.H. Jones, W. Levason, K. Minten and F.P. MacCullough, J. Chem. Soc., Chem. Commun., (1979) 736.
7 J.E. Lyons, in R. Ugo (Ed.), Aspects of Homogenous Catalysis, Vol. 3, Reidel, Dordrecht, 1977, p. 1.
8 J.E. Lyons, in M. Tsuitsui and R. Ugo (Eds.), Fundamental Research in Homogeneous Catalysis, Plenum, London, 1977, p. 1.
9 T.E. King, H.S. Mason and M. Morrison (Eds.), Oxidases and Related Redox Systems, Vols. 1 and 2, University Park Press, Baltimore, MD, 1973.
10 S. Sakaki, S. Morokuma and K. Ohkubo, Ab initio MO study of the coordination modes and bonding nature of Rh^I–N_2 complexes, J. Am. Chem. Soc., 107 (1985) 2686.
11 A. Busnot, J.F. Le Querler and J. Yazbeck, Thermochim. Acta, 197 (1992) 443.
12 A.E. Underhill and D.E. Billing, Calculations of the Racah parameters B for nickel(II) and cobalt(II) compounds, Nature, 210 (1966) 835.
13 Y. Tanabe and S. Sugano, J. Phys. Soc. Jpn., 9 (1954) 753; 9 (1954) 766.

APPENDIX

$$\mathbf{A} \xrightarrow[\text{DTA (endo) 370 K}]{\text{TG 323–398 K}}$$

$$Ni_2(Imid)_8(aspartate)_3 \text{ (WL: th. 14.8\%; exp. 15\%)} \xrightarrow[\text{DTA (endo)}]{\text{TG 398–407 K}}$$

$$Ni_2(Imid)_6(aspartate)_3 \text{ (WL: th. 11\%; exp. 10.2\%)} \xrightarrow[\text{DTA (endo) 423 K}]{\text{TG 407–444 K}}$$

$$Ni_2(Imid)_4(asparate)_2 \text{ (WL: th. 21.6\%; exp. 21.4\%)} \xrightarrow[\text{DTA (endo) 464 K}]{\text{TG 444–518 K}}$$

$2[Ni(aspartate) \cdot Imid)]$ (WL: th. 11%; exp. 11.2%) $\xrightarrow[\text{DTA (endo) 528, 580 K}]{\text{TG 518–612 K}}$

$NiCO_3 \cdot$ Ni aspartate $\cdot$ 2Imid (WL: th. 5.8%; exp. 6%) $\xrightarrow[\text{DTA (exo) 643, 694 K}]{\text{TG 612–760 K}}$

$NiCO_3 + NiO$ (WL: th. 20.3%; exp. 19.9%) $\xrightarrow[\text{DTA (exo) 760 K}]{\text{TG 660–1265 K}}$

2NiO (WL: th. 3.5%; exp. 3.8%)

Total weight loss: theoretical 88%; experimental 87.5%.

B $\xrightarrow[\text{DTA (endo) 366 K}]{\text{TG 314–406 K}}$

$Ni_2(Imid)_8(aspartate)_3$ (WL: th. 14.2%; exp. 13.7%) $\xrightarrow[\text{DTA (endo)}]{\text{TG 406–414 K}}$

$Ni_2(Imid)_7(aspartate)_3$ (WL: th. 5.5%; exp. 5.5%) $\xrightarrow[\text{DTA (endo)}]{\text{TG 414–438 K}}$

$Ni_2(Imid)_5(aspartate)_3$ (WL: th. 11.10%; exp. 10.5%) $\xrightarrow[\text{DTA (endo) 523 K}]{\text{TG 438–526 K}}$

$2[Ni(aspartate) \cdot 3Imid]$ (WL: th. 21.8%; exp. 22.7%) $\xrightarrow[\text{DTA (endo) 546 K}]{\text{TG 526–579 K}}$

$2[NI(aspartate) \cdot Imid]$ (WL: th. 11.1%; exp. 10.5%) $\xrightarrow[\text{DTA (endo) 595 K}]{\text{TG 579–644 K}}$

NiC_2O_4 + Ni aspartate $\cdot$ Imid (WL: th. 3.7%; exp. 3.5%) $\xrightarrow[\text{DTA (exo) 673 K}]{\text{TG 644–668 K}}$

$2NiCO_3$ + Imid (WL: th. 8%; exp. 7%) $\xrightarrow[\text{DTA (exo) 696 K}]{\text{TG 668–780 K}}$

$\frac{1}{2}NiO + \frac{3}{2}NiCO_3$ (WL: th. 7.3%; exp. 8.6%) $\xrightarrow[\text{DTA (exo) 1265 K}]{\text{TG 780–1265 K}}$

2NiO (WL: th. 5.4%; exp. 5.9%)

Total weight loss: theoretical 87.9%; experimental 87.9%.

C $\xrightarrow[\text{DTA (endo) 330, 424 K}]{\text{TG 318–418 K}}$

$Ni(C_5H_4NCOO)_2 \cdot$ 2Imid (WL: th. 6.8%; exp. 6.1%) $\xrightarrow[\text{DTA (endo) 585 K}]{\text{TG 418–628 K}}$

$Ni\left\langle\begin{matrix} C_5H_4NCOO \\ COOH \end{matrix}\right. \cdot$ Imid(WL: th. 30.8%; exp. 30.8%) $\xrightarrow[\text{DTA (endo) 674 K}]{\text{TG 628–677 K}}$

$NiCO_3 \cdot$ Imid (WL: th. 22.7%; exp. 23.3%) $\xrightarrow[\text{DTA (exo) 727, 752 K}]{\text{TG 677–784 K}}$

$\frac{1}{3}NiCO_3 + \frac{2}{3}NiO$ (WL: th. 20.7%; exp. 21.1%) $\xrightarrow[\text{DTA (exo) 1265 K}]{\text{TG 784–1265 K}}$

NiO (WL: th. 3.1%; exp. 3.2%)

Total weight loss: theoretical 84.1%; experimental 84.4%.

D $\xrightarrow[\text{DTA (endo) 330 K}]{\text{TG 316–448 K}}$

$Ni(C_5H_4NCOO)_2 \cdot 2Imid$ (WL: th. 6%; exp. 6.5%) $\xrightarrow[\text{DTA (endo) 584 K}]{\text{TG 448–632 K}}$

$Ni\langle^{C_5H_4NCOO}_{COOH} \cdot Imid$ (WL: th. 31%; exp. 31.7%) $\xrightarrow[\text{DTA (exo) 643 K}]{\text{TG 632–677 K}}$

$NiCO_3 \cdot Imid$ (WL: th. 22.9%; exp. 23.1%) $\xrightarrow[\text{DTA (exo) 716, 726, 737 K}]{\text{TG 677–764 K}}$

$\frac{1}{3}NiCO_3 + \frac{2}{3}NiO$ (WL: th. 20.9%; exo. 20.9%) $\xrightarrow[\text{DTA (exo) 1265 K}]{\text{TG 764–1265 K}}$

NiO (WL: th. 3.1%; exp. 2.2%)

Total weight loss: theoretical 83.9%; experimental 84.4%.

E $\xrightarrow[\text{DTA (endo) 372 K}]{\text{TG 326–392 K}}$

$NiO(Imid)_2$(*N*-acetylglycinate)$_3$ (WL: th. 15.3%; exp. 15.8%) $\xrightarrow[\text{DTA (endo) 419 K}]{\text{TG 392–413 K}}$

Ni(Imid)(*N*-acetyglycinate)$_3$ (WL: th. 12.7%; exp. 12.7%) $\xrightarrow[\text{DTA (endo) 462 K}]{\text{TG 413–465 K}}$

Ni(*N*-acetylglycinate)$_2$ (WL: th. 27.9%; exp. 27.8%) $\xrightarrow[\text{DTA (endo) 523 K}]{\text{TG 465–528 K}}$

$Ni\langle^{NH\text{–}CH_2\text{–}COOH}_{N\text{-acetylglycinate}}$ (WL: th. 6.5%; exp. 7.3%) $\xrightarrow[\text{DTA (endo) 576 K}]{\text{TG 528–617 K}}$

$Ni\langle^{COOH}_{N\text{-acetylglycinate}}$ (WL: th. 4.4%; exp. 3.9%) $\xrightarrow[\text{DTA (exo) 673 K}]{\text{TG 617–686 K}}$

NiO (WL: th. 21.9%; exp. 20.5%)

Total weight loss: theoretical 88.7%; experimental 88%.

F $\xrightarrow[\text{DTA (endo) 368 K}]{\text{TG 325–385 K}}$

$Ni_2O(\text{histidine})_6$ (WL: th. 13.5%; exp. 13.5%) $\xrightarrow[\text{DTA (endo)}]{\text{TG 385–424 K}}$

$Ni_2(\text{histidine})_5$ (WL: th. 15.1%; exp. 15%) $\xrightarrow[\text{DTA (endo)}]{\text{TG 424–460 K}}$

$2[Ni(\text{histidine})_2]$ (WL: th. 12.5%; exp. 12%) $\xrightarrow[\text{DTA (exo) 694 K}]{\text{TG 460–694 K}}$

$NiCO_3 + Ni\begin{smallmatrix}\diagup COOH \\ \diagdown \text{histidine}\end{smallmatrix}$ (WL: th. 28.8%; exp. 28.6%) $\xrightarrow[\text{DTA (exo) 701, 732, 753 K}]{\text{TG 694–1265 K}}$

2NiO (WL: th. 18.4%; exp. 18.4%)

Total weight loss: theoretical 88.3%; experimental 88.6%.

G $\xrightarrow[\text{DTA (endo)}]{\text{TG 313–352 K}}$

$Ni_2O_2(\text{Imid})_9(\text{glutarate})_3$ (WL: th. 11.9%; exp. 12.9%) $\xrightarrow[\text{DTA (endo) 452 K}]{\text{TG 352–454 K}}$

$Ni_2O_2(\text{Imid})_8(\text{glutarate})_3$ (WL: th. 5.2%; exp. 4.9%) $\xrightarrow[\text{DTA (endo)}]{\text{TG 454–520 K}}$

$Ni_2O_2(\text{Imid})_3(\text{glutarate})_3$ (WL: th. 26.1; exp. 26.2%) $\xrightarrow[\text{DTA (endo) 545 K}]{\text{TG 520–587 K}}$

2[Ni(glutarate)(Imid)] (WL: th. 17.7%; exp. 17.5%) $\xrightarrow[\text{DTA (endo) 606, 700 K}]{\text{TG 587–700 K}}$

2[Ni(glutarate)] · Imid (WL: th. 5.2%; exp. 5.3%) $\xrightarrow[\text{DTA (endo) 783 K}]{\text{TG 700–804 K}}$

$2NiCO_3$ (WL: th. 16%; exp. 15.9%) $\xrightarrow[\text{DTA (exo) 1265 K}]{\text{TG 804–1265 K}}$

2NiO (WL: th. 6.6%; exp. 5.3%)

Total weight loss: theoretical 88.3%; experimental 88.2%.

H $\xrightarrow[\text{DTA (endo) 364 K}]{\text{TG 315–402 K}}$

$Ni_2O_4(\text{Imid})_4(\text{glutamate})_4$ (WL: th. 16.5%; exp. 16%) $\xrightarrow[\text{DTA (endo) 421 K}]{\text{TG 402–439 K}}$

$Ni_2O_2(Imid)_3(glutamate)_4$ (WL: th. 8.1%; exp. 8.3%) $\xrightarrow[\text{DTA (endo) 504 K}]{\text{TG 439–520 K}}$

2[Ni glutamate] · 3Imid (WL: th. 26%; exp. 25.5%) $\xrightarrow[\text{DTA (endo) 541 K}]{\text{TG 520–578 K}}$

$2[Ni\text{–}NH_2\text{–}(COO)_2]$ · 2Imid (WL: th. 12.1%; exp. 12.2%) $\xrightarrow[\text{DTA (endo) 598 K}]{\text{TG 578–648 K}}$

$2[Ni\text{–}NH_2\text{–}(COO)_2]$ · Imid (WL: th. 5.5%; exp. 5.3%) $\xrightarrow[\text{DTA (exo)}]{\text{TG 648–856 K}}$

$NiO + NiCO_3$ (WL: th. 16.2%; exp. 15.6%) $\xrightarrow[\text{DTA (exo) 1104 K}]{\text{TG 856–1104 K}}$

2NiO (WL: th. 3.9%; exp. 5.3%)

Total weight loss: theoretical 88.3%; experimental 88.2%.